Journal of Magnetism and Magnetic Materials 560 (2022) 169424

Contents lists available at ScienceDirect

Journal of Magnetism and Magnetic Materials

journal homepage: www.elsevier.com/locate/jmmm

Research articles

Separation and trapping of magnetic particles by insertion of ferromagnetic wires inside a microchip: Proposing a novel geometry in magnetophoresis

Ali Nameni [a], Mohsen Nazari [a,*], Mohammad Mohsen Shahmardan [a], Mostafa Nazari [a], Valiollah Mashayekhi [b,*]

[a] Faculty of Mechanical and Mechatronics Engineering, Shahrood University of Technology, Shahrood, Iran
[b] Department of Electrical Engineering, Shahrood University of Technology, Shahrood, Iran

ARTICLE INFO

Keywords:
Microfluidic
Magnetophoresis
Particle separation
Particle trapping

ABSTRACT

In this study, by placing two ferromagnetic wires with different diameters inside the microchannel, a non-uniform magnetic field is generated. The magnetic force of this non-uniform field, separates different magnetic particles from each other and collects them in different parts of the channel. Using this system, we are able to collect and separate different particles from each other with an efficiency of 97%. This phenomenon depends on parameters such as wire diameter and its magnetic sensitivity, external magnetic field intensity, particle magnetic sensitivity, particle size and magnetic sensitivity of the carrier fluid. Here, these parameters are examined individually for magnetic particles (M-280 and M-450) and the optimum parameters are specified. Then, by comparing various cases, a system, for simultaneous separation and trapping is proposed. In addition, one of the magnetophoresis problems, which is interaction forces between magnetic particles investigated for the proposed system. The effects of effective parameters such as the distance between the wires and the fluid velocity are optimized to obtain maximum efficiency. Particle M-280 and M-450 are collected by wires with diameter of 100 [μm] and 50 [μm] respectively. The optimum distance between two wires is 800 [μm], so their magnetic field distribution have positive effect on each other. Also, to maximize the system efficiency the fluid velocity is set to 11 [mm/s]. By selecting these parameters as obtained values, the system efficiency is optimized. By changing wire diameter or magnetic field intensity, the proposed microchip can be used for separation and trapping of different particles.

1. Introduction

Isolation and collection of particles at micro scale, in chemical analysis [1], biological research [2], nutritional characteristics [3] and disease diagnosis [4,5] are highly permissible. Due to the special and unique properties of particles, different methods and techniques have been established for accurate and fast collection of particles. Advances in these methods make it possible to take advantage of this in separating particles or cells on a micro scale. Separation based on these methods requires smaller and less samples to perform the experimental process, which is important in reducing time and costs. Also, the smaller dimensions of the devices allow the synchronization of several processes to achieve higher purity and efficiency.

In general, all the methods and theories used for this technology is divided into active and passive categories. In passive methods, separation is done according to the structure of the channel, properties of the particles and their physical characteristics and their effects on each other, and no external force will affect it. For example, Pinched Flow [6], inertia [7], lateral displacement [8] and filtration [9] methods are among the passive methods. In contrast, in active methods, external fields in various forms are used for better separation and collection with high efficiency. Dielectrophoresis [10] Magnetoforsis [11] and Acoustophoresis [12] are examples of active methods in microfluidic systems.

Magnetophoresis is one of the active methods in which a magnetic field is used to manipulate microparticles and cells within the microchannel system [13]. Important factors in this method that affect its efficiency are magnitude and non-uniformity of magnetic field, particle or cell size, magnetic sensitivity of particles or cells, and magnetic susceptibility of solute. This method is divided into two groups of positive magnetophoresis and negative magnetophoresis.

The motion of magnetic particles inside the non-magnetic fluid is called positive Magnetoforsis and the motion of non-magnetic particles within the magnetic fluid is called negative magnetophoresis, in which

* Corresponding authors.
E-mail addresses: mnazari@shahroodut.ac.ir (M. Nazari), vmashayekhi@shahroodut.ac.ir (V. Mashayekhi).

https://doi.org/10.1016/j.jmmm.2022.169424
Received 15 July 2021; Received in revised form 15 March 2022; Accepted 27 April 2022
Available online 2 June 2022

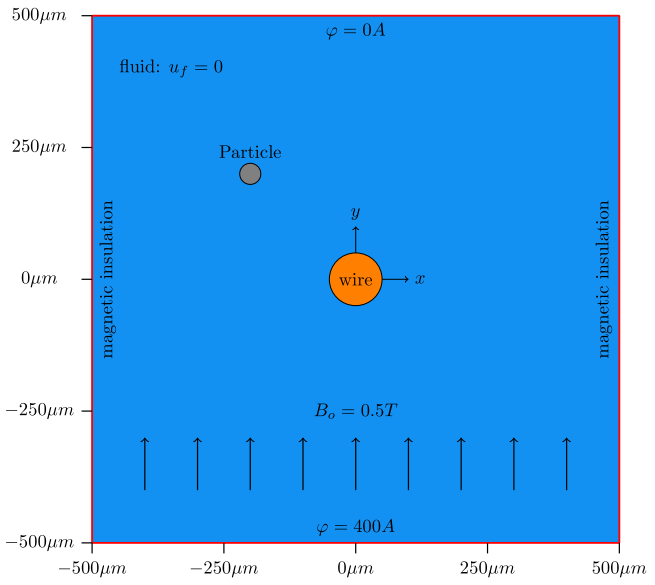

Fig. 1. Model configuration used for numerical verification analysis; $u_f = 0$, $d_w = 50$ [μm].

ferrofluid is used as a magnetic fluid. In positive magnetophoresis, magnetic particles are attracted to the high magnetic field and in negative magnetophoresis, non-magnetic particles are attracted to the low magnetic field. Magnetophoresis can be used in order to achieve a variety of purposes, including separation [14], collection [15], sorting [16], mixing [17], and concentration [18] of particles in microfluidic systems. So far, various methods and models for collecting, separating and sorting particles and cells in microfluidic systems based on magnetophoresis are proposed.

The following can be mentioned from researches in the field of particle separation based on magnetoforsis technology. Smistrup et al. [19] by designing and building a separator device, were able to separate magnetic particles with a diameter of 1 [μm] from the carrier mixture. Pamme and Wilhelm [16] have investigated separation of cancer cells from stream by labeling them using magnetic nanoparticles and using positive magnetophoresis. Kim et al. [20] with positive magnetophoresis investigated the separation of malaria-infected red blood cells from the bloodstream and to increased the efficiency of the process, they have optimized their system parameters such as microchannel height, microchannel length and flow rate. Kim et al. [21] have developed a cell separation device that can separate tumor cells from a heterogeneous mixture, such as blood. The result of their work was isolation of these cells with a yield of 82.4%.

Adams et al. [22] have developed a device for separating two magnetically labeled cell models by layering the ferromagnetic wires. The purpose of using these wires was to create a strong magnetic field gradient inside the channel. With their device, they have been able to achieve separations with a high purity of 90% and an output of 10^9 cells per hour. Zhu et al. [23] used lattice-distributed soft magnets to separate magnetic beads with efficiency more than 80%. Huang et al. [24] have collected THP-1 cells by placing a wretched layer (microwell) between the microchannel and the magnet at the top of the channel. By placing this layer, the magnetic field became more non-uniform and a local magnetic field gradient was created.

Smistrup et al. [25] used three microfabricated electromagnets in their microsystem to separate magnetic beads. Watarai and Namba [26] with addition of two iron blades to the surface of the magnets has been able to create a relatively strong magnetic field gradient at the tip of these blades and examined the collection of red blood cells in their system. Guo et al. [27] have designed a system in which using nickel ferromagnetic wires, samples were first dynamically separated and then statically collected. In this system, the collection of pathogens has been investigated.

Eshaghi et al. [28] investigated non-magnetic particle separation in a ferrofluid. They studied the motion of polystyrene particles with different sizes and effect of magnetic fields and fluid flow in a T-shape microchannel. In addition to these researches, for collection of magnetic particles using magnetic field generated by the electric current through wires, various designs have been proposed [29]. Using these electric coils, can produce large magnetic gradients and magnetic forces.

Also concentrating microparticles and cells in a narrow area of the stream is important in many microfluidic applications such as separation and collection [30]. This prevents particles from hitting the microchannel wall. In general, positive magnetophoresis is not suitable for this process because the particles tend to be attracted to the walls (magnets). However, negative magnetophoresis can be used to guide the particles to one side for better sorting [31]. Peyman et al. [32] developed a device that used two magnets to concentrate a 10 micrometer diamagnetic particles in their system. Zhu et al. [18] were able to concentrate diamagnetic particles of different sizes, which flow into the magnetic fluid, for different flow rates, using two permanent magnets.

However, microfluidic systems based on magnetophoresis have problems and disadvantages, one of which is the force of attraction between magnetic particles. This force causes the particles to be attracted to each other and form a chain of particles, which reduces the efficiency of the system. Cao et al. [33] have proposed the use of an alternating magnetic field to overcome this problem. In their system a coil is used which, by changing the direction of current in the coil, it changes the force direction between the magnetic particles and causes the particles to maintain their distance.

By investigating these researches in the field of magnetophoresis and in order to collect magnetic particles inside the microchannel, a local magnetic field gradient is needed. In this study, we used magnetic wires inside the microchannel to achieve the magnetic field gradient. Furthermore, as we want to collect two types of particles with different sizes simultaneously, so two magnetic wires with different radius are used.

In this research, we used M-280 and M-450 particles, because these particles have different sizes and have been used frequently in the literature and their properties are well known [34].

Also, by determining the radius of the effect of the particles interaction force and in order to prevent the formation of particles chain, the concentration of the solution is obtained.

2. Governing equations

The motion of a particle or cell within microfluidic systems is a function of a variety of factors. In the present microfluidic system which works by magnetophoresis technic, magnetic properties of the contents and the hydrodynamic properties of the fluid are important factors. In this system, magnetic, hydrodynamic and interparticle dipole forces are applied to the particles each of which follows its own equations. These equations can be divided into two categories, the governing equations on the fields including the magnetic field and the fluid flow field, and the governing equation on the motion of particle.

2.1. Hydrodynamic field equations

The equations governing the fluid flow field are the two equations of continuity and Navier–Stokes [35].

$$\rho_f \nabla \cdot \vec{u}_f = 0 \tag{1}$$

$$\rho_f \left(\left(\vec{u}_f \cdot \nabla \right) \vec{u}_f \right) = \nabla \cdot \sigma + F_{body} \tag{2}$$

Where ρ_f fluid density, $\vec{u}_f$ fluid velocity, σ stress tensor and F_{body} indicates the external force acting on the fluid (such as gravity).

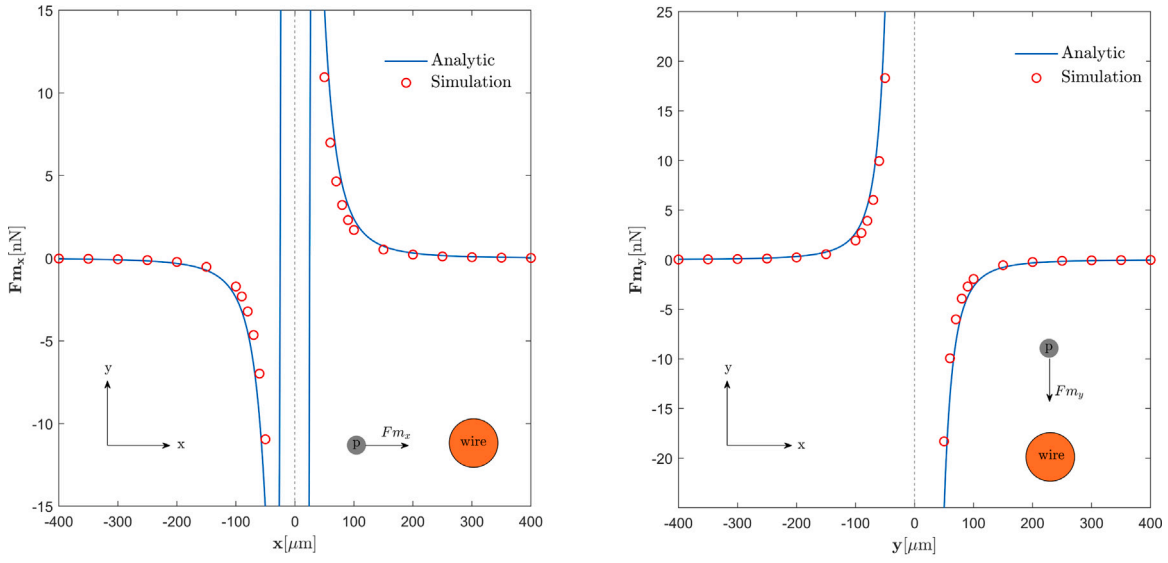

(a) F_{mx} (b) F_{my}

Fig. 2. Magnetophoresis force applied on M-280 in wire vicinity based on its distance from the wire; $B_o = 0.5$ [T], $d_w = 50$ [μm], $\mu_0 = 4\pi \times 10^{-7}$ [H/m].

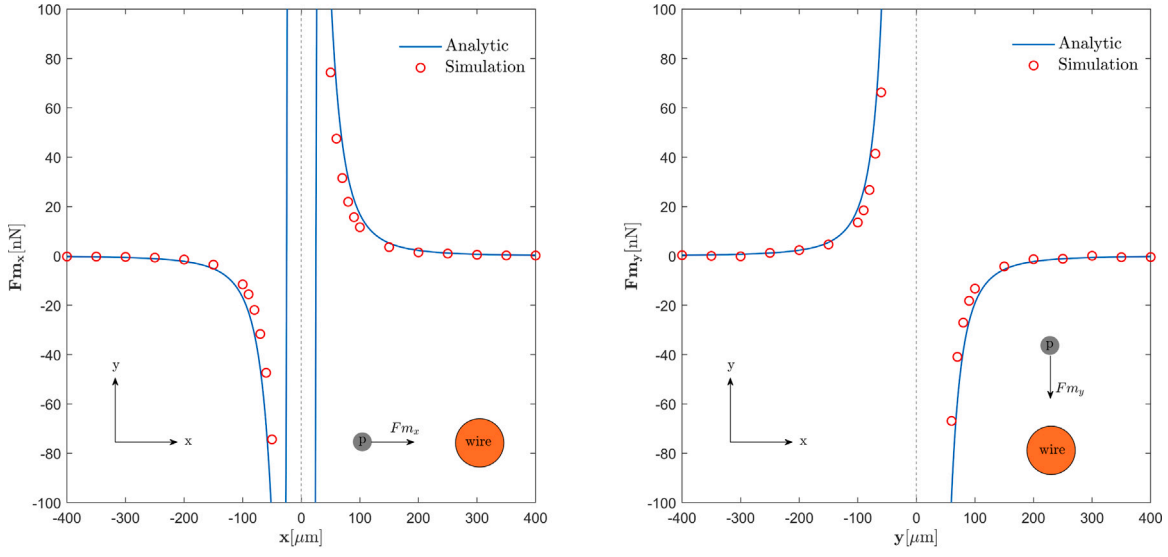

(a) F_{mx} (b) F_{my}

Fig. 3. Magnetophoresis force applied on M-450 in wire vicinity based on its distance from the wire; $B_o = 0.5$ [T], $d_w = 50$ [μm], $\mu_0 = 4\pi \times 10^{-7}$ [H/m].

2.2. Magnetic field equations

The basic equations that govern magnetic fields are generally Maxwell's equations . The general form of Maxwell's equations is as follows [36]:

$$\nabla \cdot \vec{D} = \rho_e \tag{3}$$

$$\nabla \times \vec{H} = \vec{J} + \frac{\partial \vec{D}}{\partial t} \tag{4}$$

$$\nabla \times \vec{E} + \frac{\partial \vec{B}}{\partial t} = 0 \tag{5}$$

$$\nabla \cdot \vec{B} = 0 \tag{6}$$

Assuming that the following conditions are true: the microparticles and fluids used in the micromagnetofluidic device are electrically neutral and have no electric charge, $\rho_e = 0$ so $\vec{D} = 0$, a permanent magnet is used to generate the magnetic field and no external current is applied to the microfluidic system, $\vec{J} = 0$, no voltage difference is applied to the microchannel, $\vec{E} = 0$; Maxwell's equations can be simplified as follows:

$$\nabla \times \vec{H} = 0 \tag{7}$$

According to the above relation, a quantity such as φ, which is called the magnetic scalar potential, can be defined so that the following relation holds:

$$\vec{H} = -\nabla \varphi \tag{8}$$

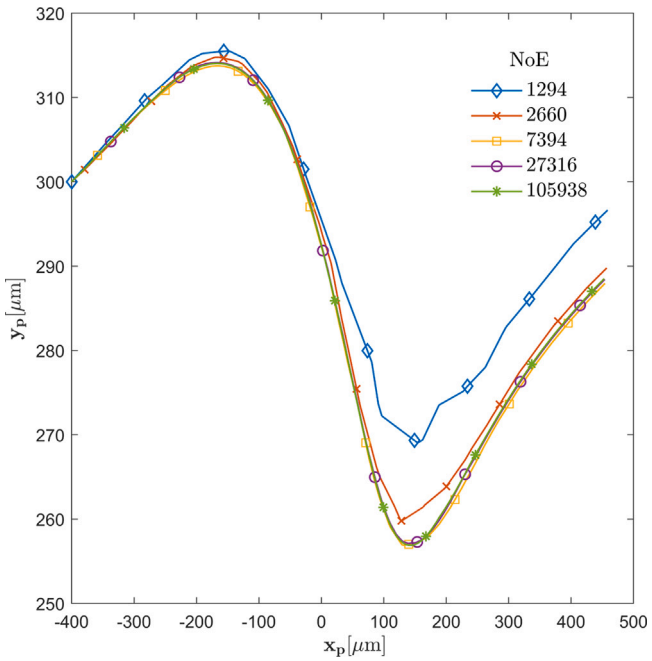

Fig. 4. Particle M-280 motion path for different grid sizes; $\bar{U}_{in} = 10\,[\mathrm{mm/s}]$, particle initial position: $(x_0, y_0) = (-400\,[\mu\mathrm{m}], 300\,[\mu\mathrm{m}])$.

2.2.1. Magnetic field around wire

Whenever a ferromagnetic wire is perpendicular to the uniform one dimensional external magnetic field, $\vec{\mathrm{H}}_o = H_o\hat{e}_y$, the magnetic potential φ around a ferromagnetic circular wire whose radius is a whose center is in the coordinates (0, 0), is defined according to the following equation [37]:

$$\varphi = -H_o y + kH_o a^2 \frac{y}{x^2+y^2},\ r = \sqrt{x^2+y^2} > a \tag{9}$$

$$k = \frac{\mu_w - \mu_o}{\mu_w + \mu_o} \tag{10}$$

In the above relation, μ_w is the magnetic permeability of the ferromagnetic wire and μ_f is the magnetic permeability of the fluid (which is approximately equal to the magnetic permeability of the vacuum, μ_0).

Using (8) and (9), the magnetic field around the ferromagnetic wire is obtained from the following equation [38]:

$$\vec{\mathrm{H}} = -\nabla\varphi = \frac{H_o}{(x^2+y^2)^2}\left[[2a^2kxy]\hat{e}_x + \left[(x^2+y^2)^2 - a^2k(x^2-y^2)\right]\hat{e}_y\right] \tag{11}$$

As can be seen in the above relation, when a ferromagnetic wire is placed vertically inside a uniform magnetic field, the field changes around wire, so that the external field becomes non-uniform and becomes two-dimensional and finds horizontal and vertical components. As a result, the magnetic field has a gradient, which causes the magnetic particles around the wire to have a magnetic force.

2.3. Particle movement equation

Consider a particle in the microchannel of a magnetophoretic device. Important forces that act on this particle are: hydrodynamic drag, magnetophoresis and interparticle forces [13]. The movement of particles in the microchannel is affected by the interaction of these forces. To determine the motion of each particle within a microfluidic channel, Newton's second law is used.

$$m_p \frac{d\vec{\mathrm{u}}_p}{dt} = \vec{\mathrm{F}}_d + \vec{\mathrm{F}}_m + \vec{\mathrm{F}}_{pp} \tag{12}$$

With m_p particle mass, $\vec{\mathrm{u}}_p$ particle velocity, $\vec{\mathrm{F}}_m$ magnetophoresis force, $\vec{\mathrm{F}}_d$ drag force and $\vec{\mathrm{F}}_{pp}$ as particles magnetic interaction force. Other forces such as gravity and lift and buoyancy are neglected, as a result, they have no impact on particles lateral displacement.

2.3.1. Hydrodynamic drag force

Large particle. If we consider the particles as large particles, the hydrodynamic drag force applied on them is calculated according to the following equation [39].

$$\vec{\mathrm{F}}_d = \int \left[-\mathrm{P}I + \eta_f(\nabla\vec{\mathrm{u}}_f + (\nabla\vec{\mathrm{u}}_f)^T)\right]\cdot \hat{\mathrm{n}}\mathrm{d}A \tag{13}$$

Where P is pressure, I is identity matrix, $\hat{\mathrm{n}}$ is surface outward normal vector and A is the particle surface.

Point particle. For microparticles located within microchannels with a low Reynolds number, the drag force is given by the Stokes relation and the relative velocity of the particles [13].

$$\vec{\mathrm{F}}_d = 6\pi\eta_f r_p(\vec{\mathrm{u}}_f - \vec{\mathrm{u}}_p)C_w \tag{14}$$

Where r_p is the particle radius and $\vec{\mathrm{u}}_f$ and $\vec{\mathrm{u}}_p$ are fluid and particle velocity respectively. Also C_w is a constant used to exert the effect of wall on the drag force on microparticles [13].

$$C_w = \left[1 - \frac{9}{16}\left(\frac{d_p}{d_p+2\delta_w}\right) + \frac{1}{8}\left(\frac{d_p}{d_p+2\delta_w}\right)^3 - \frac{45}{256}\left(\frac{d_p}{d_p+2\delta_w}\right)^4 - \frac{1}{16}\left(\frac{d_p}{d_p+2\delta_w}\right)^5\right]^{-1} \tag{15}$$

where δ_w is the distance of particles from microchannel wall.

2.3.2. Magnetophoresis force

Large particle. If we consider the particles as large particles, the magnetic force applied on them is calculated using the Maxwell stress tensor according to the following equation [40]:

$$\vec{\mathrm{F}}_m = \int \left[-\frac{1}{2}(\vec{\mathrm{H}}.\vec{\mathrm{B}}) + \vec{\mathrm{H}}\vec{\mathrm{B}}^T\right]\cdot \hat{\mathrm{n}}\mathrm{d}A \tag{16}$$

Where $\vec{\mathrm{H}}$ is the magnetic field intensity, $\vec{\mathrm{B}}$ is the magnetic flux density, $\hat{\mathrm{n}}$ is the outward surface normal vector and A is the particle surface.

Point particle. If a magnetic particle is considered as a point magnetic dipole, the magnetic force acting on it is equal to [38]:

$$\vec{F}_m = \frac{1}{2}\mu_o\chi V_p \nabla\vec{\mathrm{H}}^2 \tag{17}$$

Due to the magnetic field within the microchannel near the wire (11) the horizontal and vertical components of the magnetic force are obtained from the following equations [38]:

$$F_{mx} = -2\mu_o\chi V_p H_o^2 a^2 k\frac{(ka^2 - x^2 + 3y^2)x}{(x^2+y^2)^3} \tag{18}$$

$$F_{my} = -2\mu_o\chi V_p H_o^2 a^2 k\frac{(ka^2 - 3x^2 + y^2)y}{(x^2+y^2)^3} \tag{19}$$

Where in these relations: $\vec{\mathrm{H}}_o = H_o\hat{e}_y$ external magnetic field intensity (that is in y direction), a ferromagnetic wire radius and k is a function of wire magnetization saturation, M_{ws}, is defined according to the following relation [38]:

$$k = \begin{cases} 1.0, & \text{if } H_o \le \frac{M_{ws}}{2}; \text{(non-saturated)} \\ \frac{M_{ws}}{2H_o}, & \text{if } H_o > \frac{M_{ws}}{2}; \text{(saturated)} \end{cases} \tag{20}$$

The above equations show that the magnetic force applied to the particles is a function of their location, and this force changes as their distance from the wire changes.

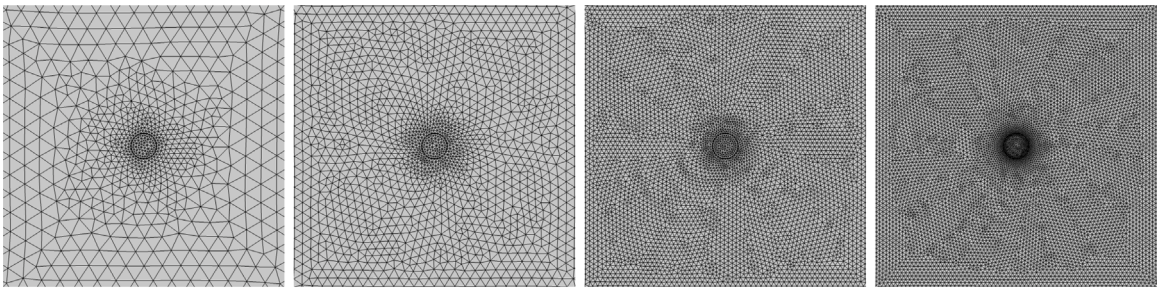

(a) Case I (b) Case II (c) Case III (d) Case IV

Fig. 5. Grid structure around wire; (a) 2660 elements, (b) 7394 elements (c) 27316 elements (d) 105938 elements. More details listed in Table 2.

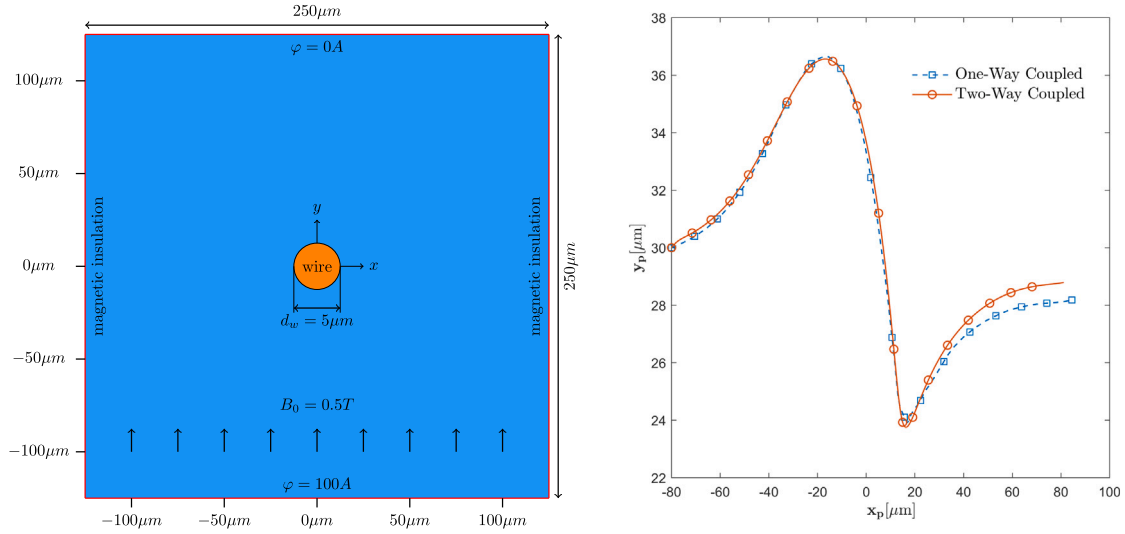

(a) Model configuration (b) Particle motion path

Fig. 6. Comparison between large particle and point particle assumption (one way and two way coupled) for a single M-280 particle; $\bar{U}_{in} = 10\,[\mathrm{mm/s}]$.

Table 1
Definition and quantity of parameters.

Parameter		Value	Definition
wires	μ_w	100000	wires magnetic permeability
	M_{ws}	8.6×10^5	wire's saturation magnetization
M-280	d_p	2.8 [μm]	particle diameter
	ρ_p	1578 [kg/m^3]	particle density
	μ_p	1.923	particle relative permeability
M-450	d_p	4.5 [μm]	particle diameter
	ρ_p	1538 [kg/m^3]	particle density
	μ_p	2.58	particle relative permeability
fluid	ρ_f	1000 [kg/m^3]	fluid density
	η_f	0.001 [Pa s]	fluid dynamic viscosity
	μ_f	1	fluid relative permeability

3. Numerical model verification

In this study, COMSOL® 5.3a software is used to solve the equations which is available in our laboratory of advanced numerical simulation and trace particles numerically. In order to model the motion of microparticles within a magnetophoresis system, first of all, forces and fields need to be calculated accurately.

Here, to measure the validity of the obtained results, they are compared with the existing analytical relations and error is determined. This comparison is made for the magnetic force acting on a particle.

3.1. Analytical magnetophoresis force

To obtain the analytical magnetophoresis force consider a ferromagnetic wire perpendicular to the external uniform magnetic field. The components of this force are obtained using (18) and (19) relations.

By substituting $y = 0$ and $x = 0$ in (18) and (19) respectively and using Table 1 values, magnetic force components are obtained for each particle M-280 and M-450, in terms of particle distance from the wire.

3.2. Numerical magnetophoresis force

To calculate MAP force, we modeled system showed in Fig. 1. With given boundary condition, (8) is solved time independently and in a steady state then, distribution of magnetic field within the system is obtained. Once the field distribution is known, the force acting on the particle is calculated. Changing particle position and repeating this process, gives MAP force based on particle position.

3.3. Analytical and numerical force comparison

Calculated MAP force is shown in Figs. 2 and 3 for M-280 and M-450 respectively. As can be seen, the results of the numerical model has an error of 97% and it can be concluded that the simulation of the numerical model is acceptable and reliable.

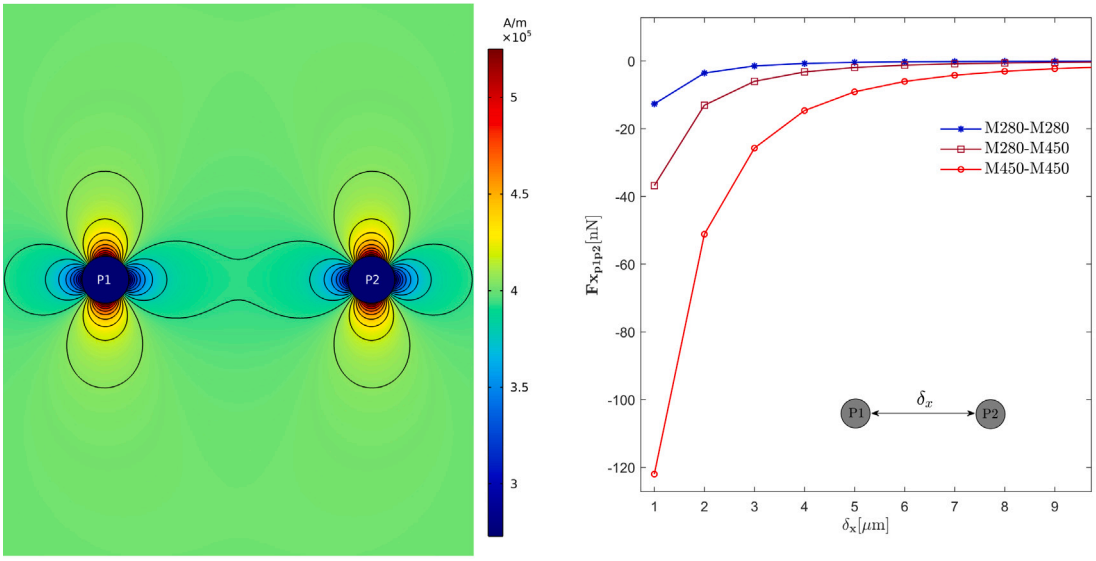

(a) H and $H{=}cte$ lines around two particles in horizental placement configuration

(b) Magnetic force between two particles in horizental placement configuration

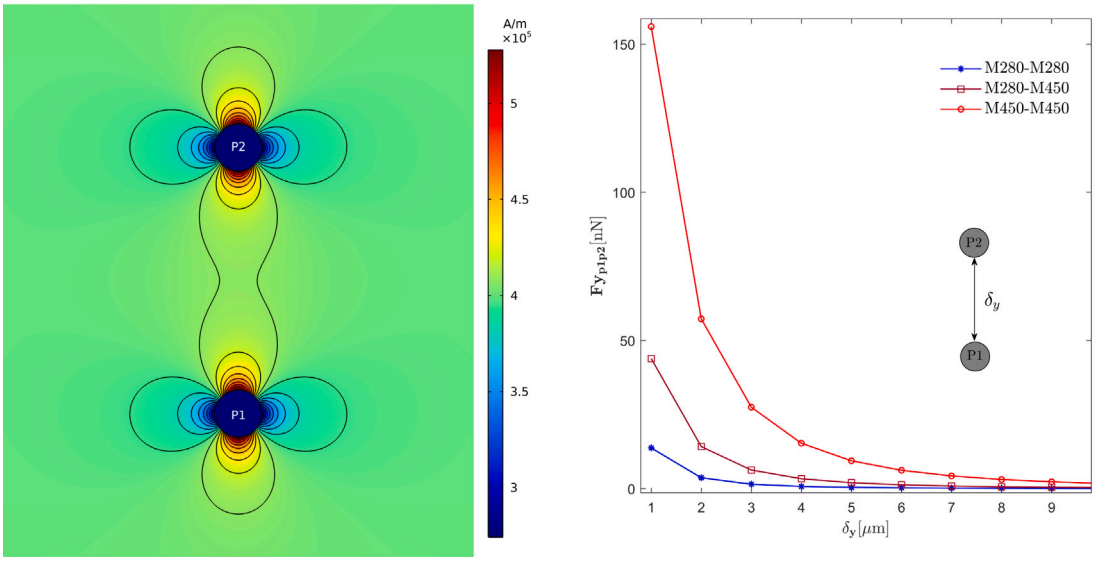

(c) H and $H{=}cte$ lines around two particles in vertical placement configuration

(d) Magnetic force between two particles in vertical placement configuration

Fig. 7. Magnetic interaction force between two particles in various configurations (force applied on P2 from P1); $\bar{U}_{in} = 0$, $B_o = 0.5$ [T].

4. Grid independency

Grid generation directly affects the results of numerical analysis and cannot be ignored. Therefore, one of the steps of simulation and analysis of numerical model is to examine the dependency of the results on the generated grid or so-called grid study. To investigate the independence of the results from the grid size, the motion of a particle (M-280) for 5 different sizes of grids, was compared. Results are shown in Fig. 4. Also these grids features are listed in Table 2 and their structures are shown in Fig. 5.

Table 2
Grids features.

Case number	Minimum element size [μm]	Maximum element size [μm]	Number of elements
I	0.125	37	2660
II	0.075	20	7394
III	0.02	10	27316
IV	0.015	5	105938

5. Simulation method

In this research, two basic assumptions have been used. The first assumption is that the effect of particles on the magnetic field and the fluid flow field is negligible, and the second assumption is to ignore the effect of the particles on each other.

5.1. Point particles

This assumption causes the equations of fields and particle motion to be one way coupled, i.e. first fluid flow field and magnetic field are solved stationary and independent of the presence of particles, and

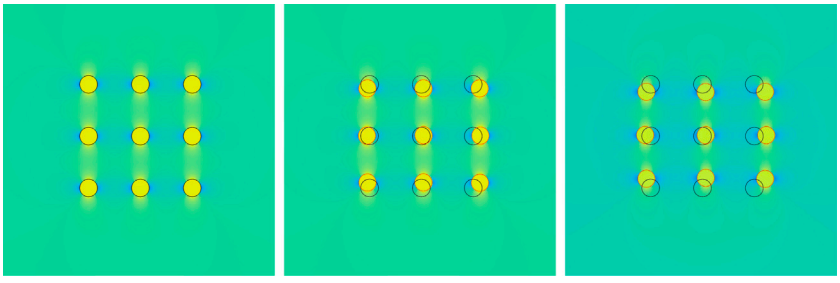

(a) $t = 0$ [s] (b) $t = 20$ [μs] (c) $t = 30$ [μs]

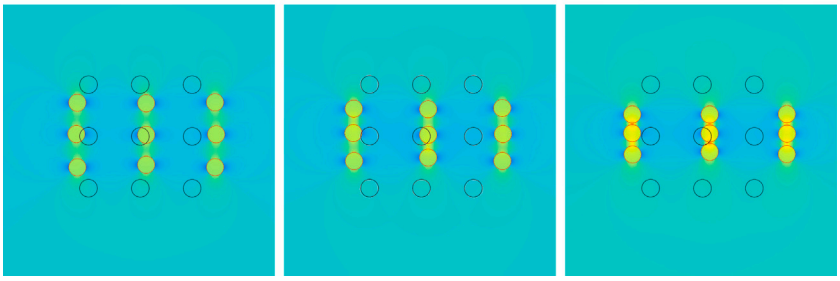

(d) $t = 50$ [μs] (e) $t = 55$ [μs] (f) $t = 60$ [μs]

Fig. 8. Effect of interparticle magnetic force on set of M-280 particles (initial position and current position are shown in black and red circles respectively); $B_o = 0.5$ [T], $\bar{U}_{in} = 10$ [mm/s], $\delta_x = \delta_y = 10$ [µm].

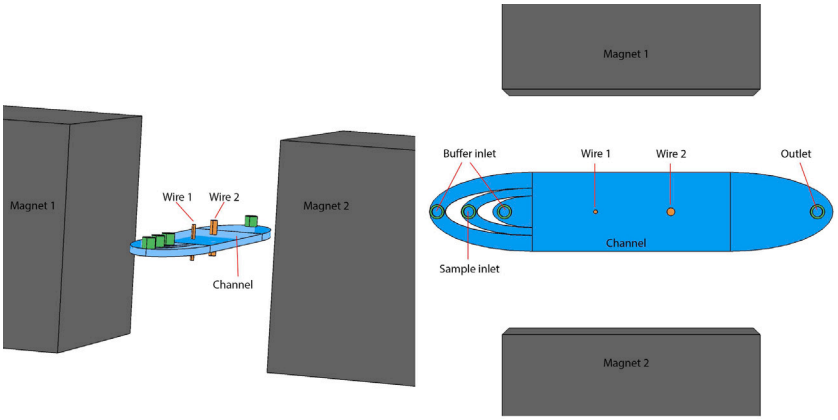

(a) 3D view (b) Top view

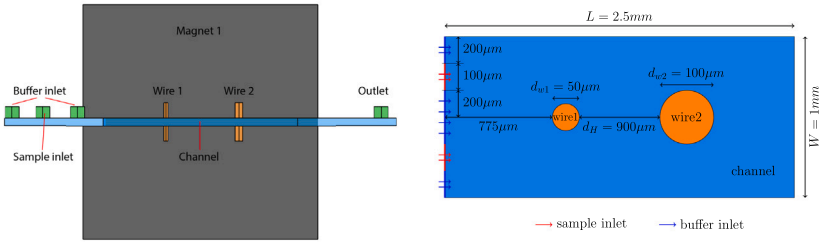

(c) Side view (d) Geometric dimensions

Fig. 9. Microfluidic system from different views and its geometric dimensions.

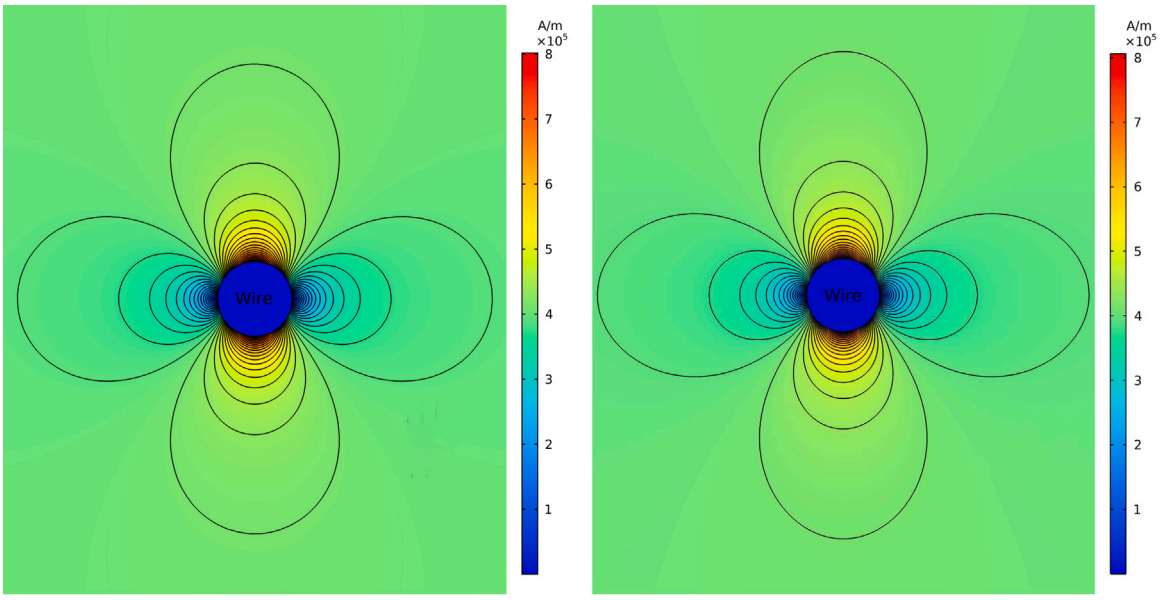

(a) $d_w = 50\,[\mu\mathrm{m}]$ (b) $d_w = 100\,[\mu\mathrm{m}]$

Fig. 10. H and $H = cte$ lines around wire for two different wire diameter; $B_o = 0.5\,[\mathrm{T}]$.

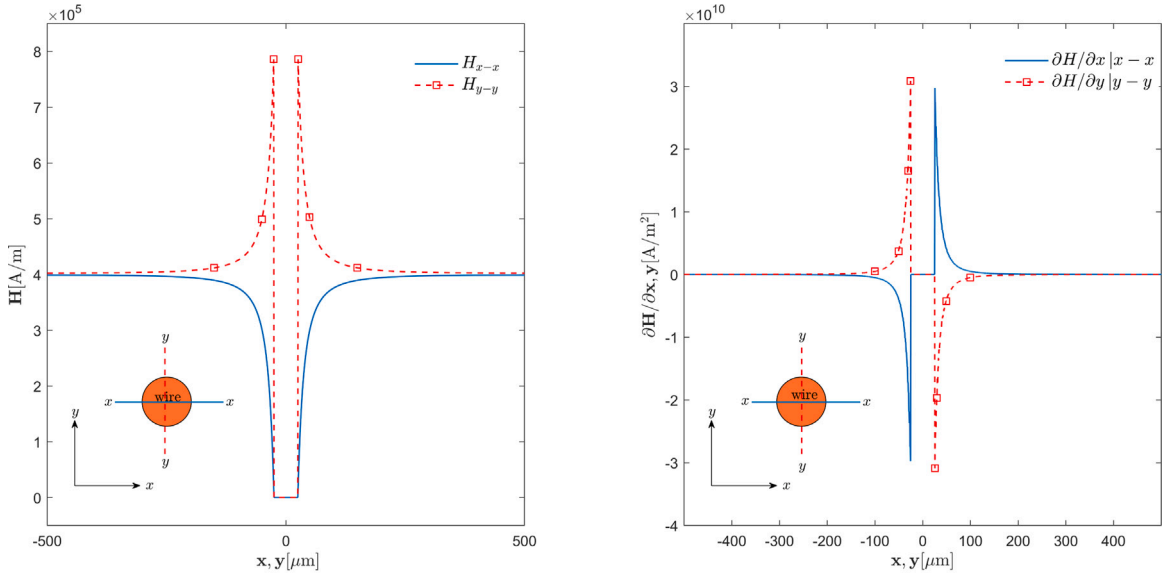

(a) H (b) $\partial H/\partial x, y$

Fig. 11. Magnetic field intensity and its gradient in x and y directions across wire; $B_o = 0.5\,[\mathrm{T}]$, $d_w = 50\,[\mu\mathrm{m}]$.

the fluid velocity and the magnetic field distribution within the microchannel are obtained. The magnetic and drag forces on the particle are calculated at any point within the channel using (14) and (17) respectively. Then, using the values of these forces, the particle motion equation is solved time dependent. By repeating this process, the path of the particle within the channel is obtained.

On the other hand, when the assumption of point particle is not taken into account, so-called two-way coupling, the fields equations and the particle motion equation are not independent of each other and all equations are solved simultaneously and time dependently. In the two-way coupling, the geometry of the particles is modeled and to calculate the forces, the stress tensors are integrated on the particle surface.

To validate this hypothesis, a special case in which only one M-280 particle is released into the flow, with certain parameters, was first modeled by one-way coupling method and the particle trajectory was obtained. Then, under the same condition it was modeled by the two-way coupling method and the particle path was obtained. The results of these models are compared with each other and showed in Fig. 6. The results show that due to the small size of the particles relative to the dimensions of the system, the assumption of point particles is acceptable with 96% accuracy.

5.2. Interparticle magnetic force

In this research, the magnetic force between the particles is neglected. When the particles concentration is low and the particles are relatively far apart, this force is negligible and can be ignored. But if the number of particles and their concentration is high, this force

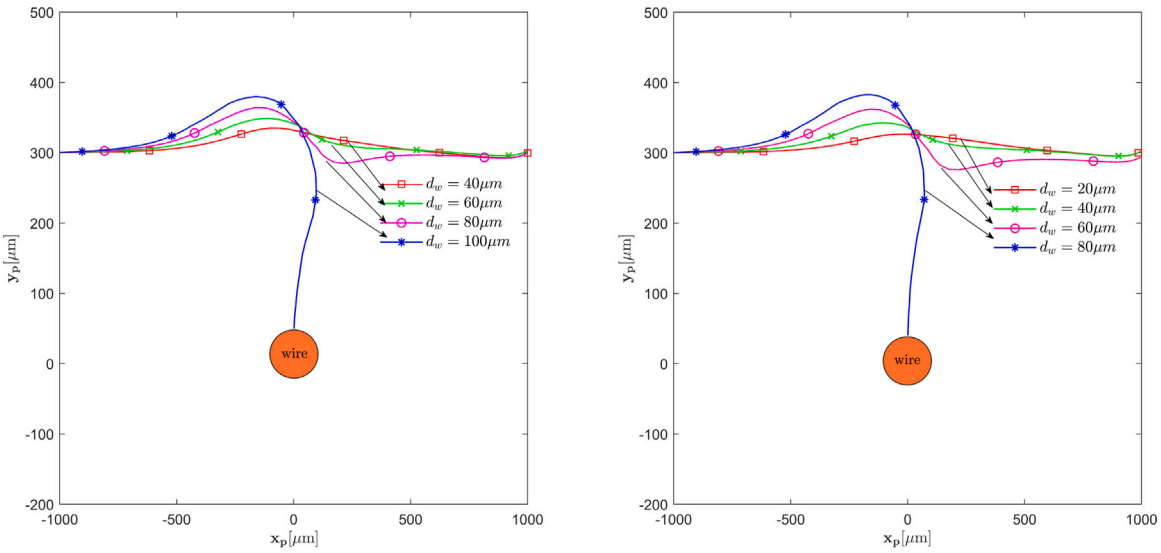

(a) Particle M-280 (b) Particle M-450

Fig. 12. Effect of wire diameter (four different sizes) on the particle motion path; $\bar{U}_{in} = 10\,[\text{mm/s}]$, $B_o = 0.5\,[\text{T}]$.

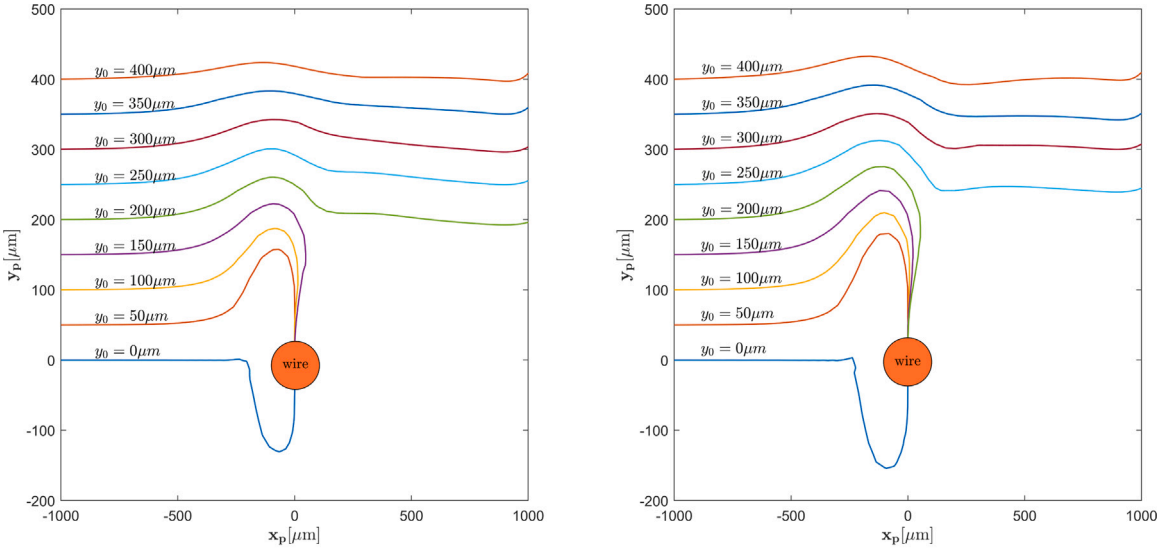

(a) Particle M-280 (b) Particle M-450

Fig. 13. Particle motion path for different initial release position; $\bar{U}_{in} = 10\,[\text{mm/s}]$, $d_w = 50\,[\mu\text{m}]$, $B_o = 0.5\,[\text{T}]$.

is important and cannot be ignored. Due to the difference between particles and fluid magnetic properties, magnetic particles act like a magnetic wire, making the uniformity of the magnetic field non-uniform around them. This magnetic field gradient around particles, creates a force field around them; which is activated at short distances. This force value, is shown in Fig. 7 for different placement of particles M-280 and M-450 relative to each other.

The motion of a set of 9 M-280 particles that were $10\,[\mu\text{m}]$ apart from each other, by considering interparticle magnetic force and using two-way coupled model, was also examined. Fig. 8 shows the motion of these particles over a short period of time. It is observed that the particles after a short time, in the vertical direction, they approach each other and stick together and in the horizontal direction they are separated from each other. From Fig. 7, it can be seen that the effected area of this force is small. For particle M-280 this area has a radius of $7\,[\mu\text{m}]$ and for particle M-450 it has a radius of $10\,[\mu\text{m}]$. Also the sign of this force shows that particles under the effect of this force are attracted to each other in the vertical direction (form particles chain) and repelled from each other in the horizontal direction. Knowing the area of effect of this force, the concentration of the particles solution is chosen in such a way that the particles are far enough apart so this force does not get activated along their path.

6. System configuration

Fig. 9 shows the micromagnetofluidic system designed here, for simultaneous separation and collection of two magnetic particle models. In this system, a permanent magnet is used to create magnetic field, and to create local magnetic field gradient, two nickel ferromagnetic wires, with different diameter, are placed inside the microchannel. The first wire with smaller diameter, W1, is used to collect larger particles, M-450, and the second wire, W2, with larger diameter is used to collect smaller particles, M-280.

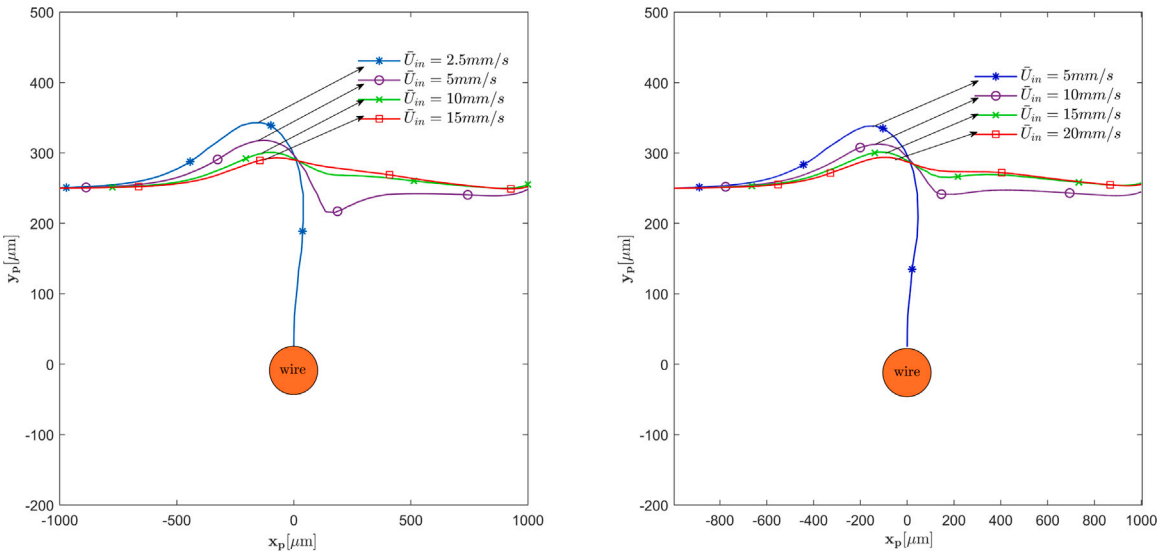

(a) Particle M-280 (b) Particle M-450

Fig. 14. Motion of particles for different fluid inlet velocities; $y_0 = 250\,[\mu m]$, $d_w = 50\,[\mu m]$, $B_o = 0.5\,[T]$.

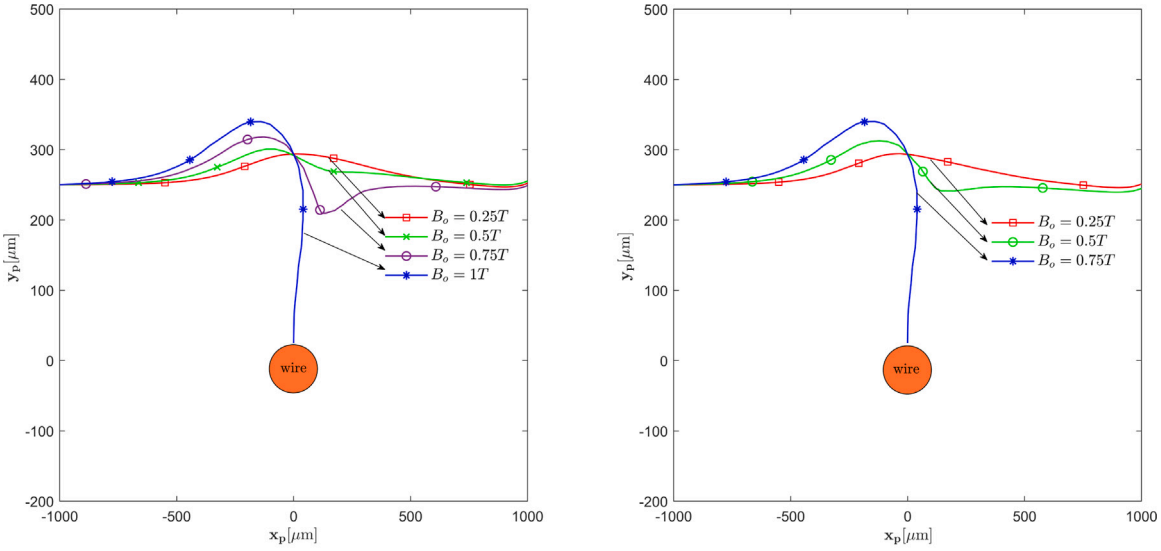

(a) Particle M-280 (b) Particle M-450

Fig. 15. External magnetic field effect on particle displacement; $\bar{U}_{in} = 10\,[mm/s]$, $y_0 = 250\,[\mu m]$, $d_w = 50\,[\mu m]$.

Through the depth of the channel, magnetic field and flow field are relatively uniform and there are no force applied to the particles, so there is no particle movement in this direction. Also, the depth of channel is 100 [μm], but the system is modeled in 2D with this assumption that particles are far away from top and bottom of the channel (in the center of depth).

7. System performance

Distribution of a magnetic field within a material is a function of magnetic permeability of that material, so, since the ferromagnetic wires have a much larger magnetic permeability than the particle-carrying fluid (which in this study is water), magnetic field distribution near these wires comes out of uniformly and finds a strong gradient locally.

Magnetic field distribution around a wire is shown in Fig. 10. It can be seen that on the left and right of the wire, the magnetic field is minimum and at the top and bottom of the wire, the magnetic field is maximum.

The interaction of magnetic force and drag force determines the efficiency of this system. If the magnetic force is greater than the drag force, particles will accumulate on the wires, otherwise they will pass through the channel. (14) shows that the hydrodynamic drag force increases with increasing particle size or particle velocity relative to the fluid. Also (17) shows that the magnetic force is directly related to the magnetic field gradient, particle size and its magnetic permeability. Therefore, due to the fact that the particles M-450 are larger in size and have a greater magnetic permeability than particles M-280, it results in greater hydrodynamic and magnetic force being applied to them.

Figs. 11(a) and 11(b) show the intensity of the magnetic field and its gradient, in the horizontal and vertical directions, respectively. From Fig. 11(b) can be seen that on the left side of the wire and upstream of the flow, the magnetic gradient sign is negative, which by passing

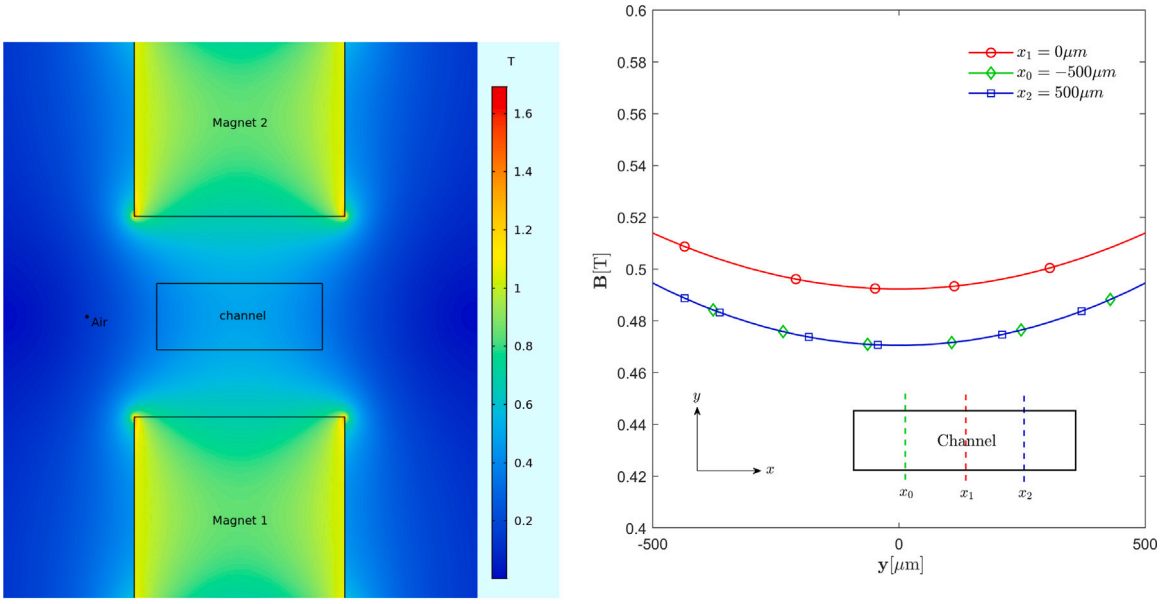

(a) B (b) B in three section of the channel

Fig. 16. Magnets placement and resulting magnetic field inside channel.

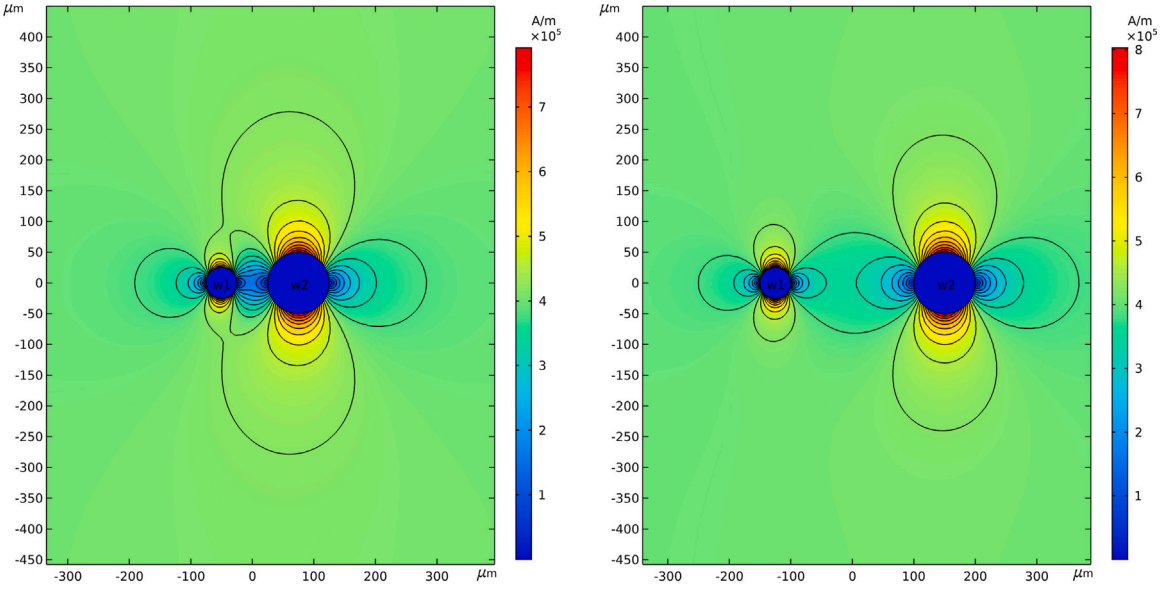

(a) $d_H = 50\,[\mu\text{m}]$ (b) $d_H = 200\,[\mu\text{m}]$

Fig. 17. Magnetic field distribution around two wires; $u_f = 0$, $d_{w1} = 50\,[\mu\text{m}]$, $d_{w2} = 100\,[\mu\text{m}]$, $B_o = 0.5[\text{T}]$.

through the wire, on the right side, the magnetic gradient sign changes and becomes positive. Since according to the relation of magnetic force, (17), the force sign is the same as the sign of magnetic field gradient, it is concluded that the magnetic force on the left and right of the wire is the repulsive force and removes the particles from the wire. In contrast, the magnetic gradient above the wire is positive and below the wire it is negative, causing attractive force to be applied on particles, therefore particles move toward the wire. This attractive force is called particles trapping factor. Using this theory, we placed a wire with small diameter to collect large particles at the beginning and a wire with large diameter to collect small particles at the end of the channel.

8. Results analysis

As mentioned, in our proposed device, two ferromagnetic wires were used to create a strong magnetic gradient inside the channel so that particles could be separated and collected using the magnetic force that this gradient exerts on them. We have investigated the important parameters involved in this system. To do this, first a system in which only one wire is in the center of the channel is considered, then its parameters, which include the wire diameter, particle release location, fluid flow velocity and magnetic field strength are studied in order to trap each particle. Then a system with two wires is used to study the effect of distance between the wires. Finally, the efficiency of the

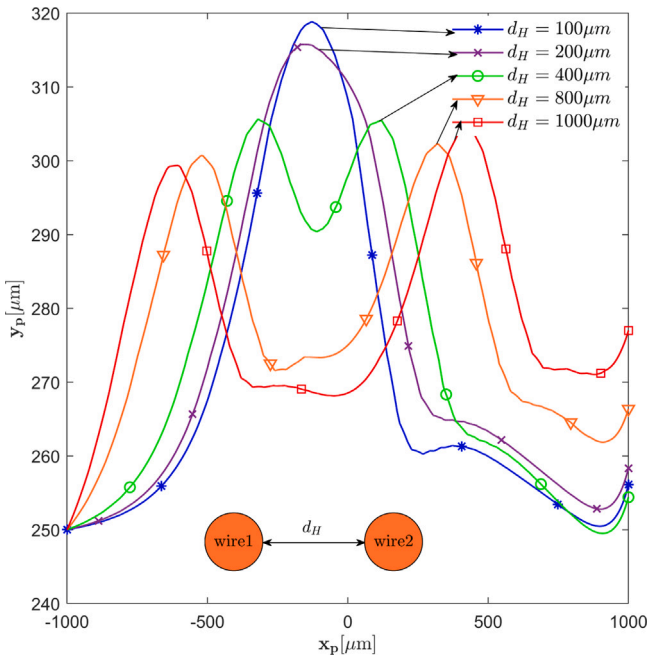

Fig. 18. M-280 vertical displacement and its motion path through channel for various distances between wires, d_H; $\bar{U}_{in} = 10\,[\text{mm/s}]$, $y_0 = 250\,[\mu\text{m}]$, $d_{w1} = 50\,[\mu\text{m}]$, $d_{w2} = 100\,[\mu\text{m}]$.

wires for this system is calculated and its value in terms of the distance between the wires and the flow rate of the fluid is obtained.

8.1. Single wire analysis

8.1.1. Wire diameter

One of the important parameters in this system that has a great effect on the microparticles displacement is the wire diameter. Fig. 12 shows the motion of a single particle for wires with different diameters. It is observed that as the diameter of the wire increases, the magnetic force applied to the particle increases due to the increase of the magnetic field gradient. As the particle approaches the wire from the left, it is first in the repulsion region of the wire, also because the velocity of the fluid has a component in the y direction, the particle moves slightly upwards. By moving in the direction of the channel, it enters the attraction area of the wire and moves toward the wire. In wires with small diameters, the magnitude of the magnetic force is small compared to the hydrodynamic force, and the particle has a small displacement in the vertical direction, but as the diameter of the wire increases, the magnetic force on the particle increases and causes the particle to move vertically more. This increase in wire diameter continues until the magnetic force on the particle is large enough to overcome the fluid hydrodynamic force, and as a result, the particle could not leave the attractive field of the wire and is collected on the surface of the wire. As shown in Fig. 12, the critical diameter of the wire for trapping particle M-280 is equal to 100 [μm] and for particle M-450 is equal to 80 [μm].

8.1.2. Particle release position

Depending on where the particles are in the vertical direction of the channel, different hydrodynamic forces are applied to them. Also the magnetic force on the particles, changes with the displacement of the particles. Therefore, the movement of microparticles within the microchannel can be considered as a function of their initial release position. Particle motion for different initial release position for the two particles models under consideration, is shown in Fig. 13. It can be seen that if M-280 particles are released in the range of 0 to 200 [μm] from the center of the channel at the inlet, they can be trapped with this wire diameter. This interval for particle M-450 is from 0 to 350 [μm].

8.1.3. Fluid inlet velocity

Hydrodynamic force is one of the most important forces in the microfluidic systems. This force is due to the velocity difference between the fluid and the particle, so that this force increases with increasing velocity of the fluid. Fig. 14 shows the motion of particles within a microchannel for different inlet velocities. As a result, the M-280 particle can be collected at velocities less than $\bar{U}_{in} = 2.5\,[\text{mm/s}]$ and the M-450 particle at velocities less than $\bar{U}_{in} = 15\,[\text{mm/s}]$ for the specified wire diameter.

8.1.4. External magnetic field

In magnetophoresis-based systems, magnetic force plays the most important role in achieving the goal of the system. This force depends on the external magnetic field applied to the system. As can be seen from Fig. 15, M-280 particle needs stronger field to be absorbed by the wire due to its smaller size ($B_o = 1\,[\text{T}]$), but M-450 particle with larger size can be collected in weaker fields ($B_o = 0.5\,[\text{T}]$). In this research, a permanent magnet has been used to create an external magnetic field. Also, in order to external field be uniform, two magnets are used on the sides of the channel so that the opposite poles face each other. This, not only intensifies the field, but also distributes it evenly. Permanent magnet B222G-N52 (Kjmagnets), $1/8\,[\text{in}] \times 1/8\,[\text{in}] \times 1/8\,[\text{in}]$ with magnetization $\vec{\text{M}} = M\hat{e}_y = 1.18 \times 10^6\,[\text{A/m}]$ is selected. Given that the external field is considered $B_o = 0.5\,[\text{T}]$, when distance from center of each magnet to the center of channel is 3.1 [mm], the required field is created, which is quasi-uniform. This field can be seen in Fig. 16.

8.2. Pair wires analysis

Depending on the diameter of the wires and their distance from each other, the effect of the wires on the magnetic field of the other wire will be different. Fig. 17 shows magnetic field distribution and $H = cte$ lines, with first wire diameter 50[μm] and second wire diameter 100 [μm] (this diameters are selected based on section "Single wire diameter analysis" results) in two different wires distances. It is observed that by increasing the distance between the wires, their effect on each other decreases to the extent that the effect of each wire on the magnetic field becomes independent of the presence of the other wire.

8.2.1. Distance between wires

Motion of a particle M-280 for different distances between wires is shown in Fig. 18. When the distance between wires is small and the wires are close to each other, the magnetic field around each wire affects the magnetic field around the other wire, and the magnetic force on the particle intensifies relative to the single-wire state. At small distances, it is observed that the effect of two wires is like the effect of a wire with a larger diameter and the motion of the particle has one peak. It is observed that as the distance between the wires increases, their effect on each other decreases and the particle motion diagram finds two peaks; until this effect disappears and each wire operates independently and the particle is not affected by the other wire when it reaches each of the wires.

8.2.2. Particles set motion

Consider the motion of a set of particles inside a channel with two wires. As the particles move through the channel, they first reach the small wire (large enough to trap M-450 particles), and M-450 particles, because they are larger in size, do not pass through the wire and they are gathered around it. M-280 particles, which are smaller in size and have a smaller magnetic force, pass through the first wire and move toward the second wire. The second wire is larger in diameter than the first wire so magnetic gradient around it is stronger. As a result,

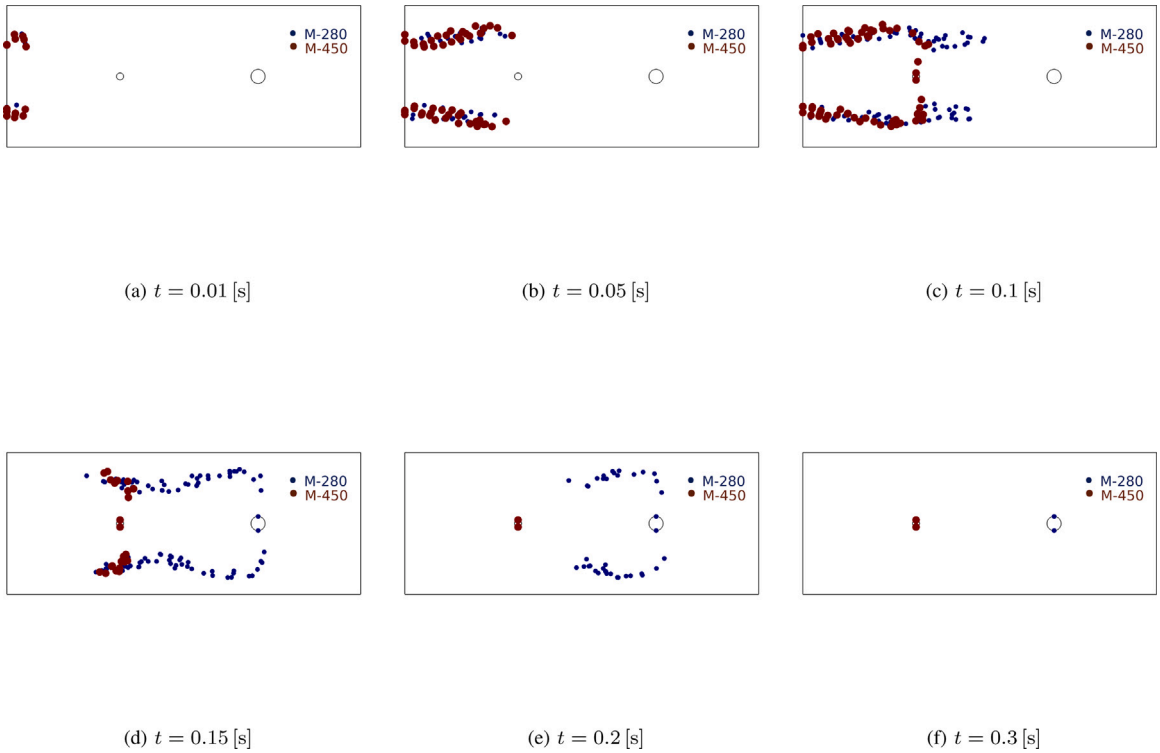

(a) $t = 0.01$ [s] (b) $t = 0.05$ [s] (c) $t = 0.1$ [s]

(d) $t = 0.15$ [s] (e) $t = 0.2$ [s] (f) $t = 0.3$ [s]

Fig. 19. Motion of particles set (blue: M-280, red:M-450); $\bar{U}_{in} = 10$ [mm/s], $B_o = 0.5$ [T], $d_{w1} = 50$ [μm], $d_{w2} = 100$ [μm].

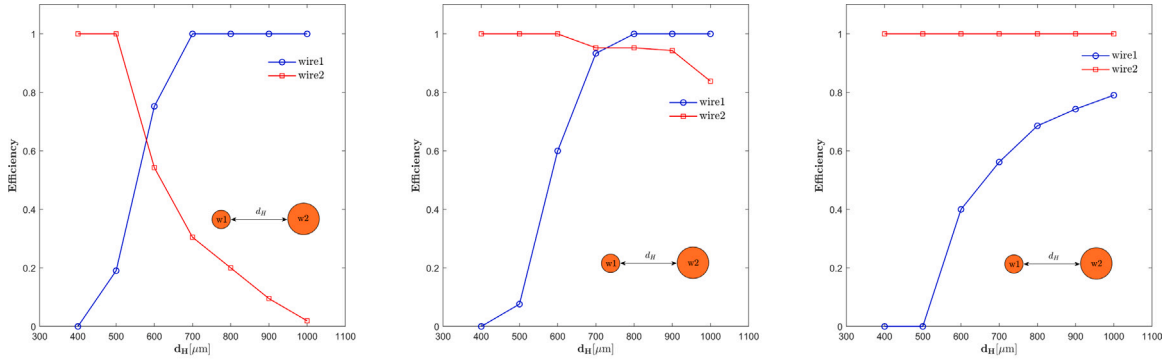

(a) $\bar{U}_{in} = 5$ [mm/s] (b) $\bar{U}_{in} = 10$ [mm/s] (c) $\bar{U}_{in} = 15$ [mm/s]

Fig. 20. Trap efficiency of each wire by distance between them; $B_o = 0.5$ [T]$d_{w1} = 50$ [μm], $d_{w2} = 100$ [μm].

stronger force is applied to small particles (M-280). This wire is considered to be large enough so, the resulting magnetic force is sufficient to overcome the hydrodynamic force and causes the absorption and accumulation of smaller particles around it.

The motion of a set of particles in a system in which the diameter of the first wire is 50 [μm] and the diameter of the second wire is 100 [μm], is shown in Fig. 19 versus time. In this model, particles from two inlets, each 100 [μm] wide, as shown in Fig. 9(d), are released into the fluid. How these particles are released at the inlets is defined as follows: at $t = 0$ [s] started and each 0.005 [s], 5 of each particle (M-280, M-450) with random distribution is released in to the fluid by time $t = 0.1$ [s].

8.3. Efficiency

Here we define the efficiency for ferromagnetic wires. The efficiency of the first wire means the ratio of number of particles M-450 collected by this wire to the total number of particles M-450 released into the microfluidic system, also the efficiency of the second wire is the ratio of number of particles M-280 collected by this wire to the total number of particles M-280 released into the system. According to the model of previous section, 105 of each of the M-280 and M-450 particles are released into the system. Efficiency of each wire is calculated by counting number of particles trapped by each wire and divided by this number.

8.3.1. Efficiency based on wires distance

The efficiency of wires is calculated as a function of the distance between them for three different fluid inlet velocities and is plotted in Fig. 20. It is observed that if the distance between the two wires is small, the first wire will have a very low efficiency. At a distance less than 400 [μm], the efficiency of the first wire is zero, which means that no particle is collected on the first wire. As the distance increases, it is observed that the efficiency of first wire also increases, and this is because the effect of second wire on the magnetic field of first wire decreases. But as the distance between the wires increases from a certain value (500 [μm] for inlet velocity of 5 [mm/s] and 500 [μm] for

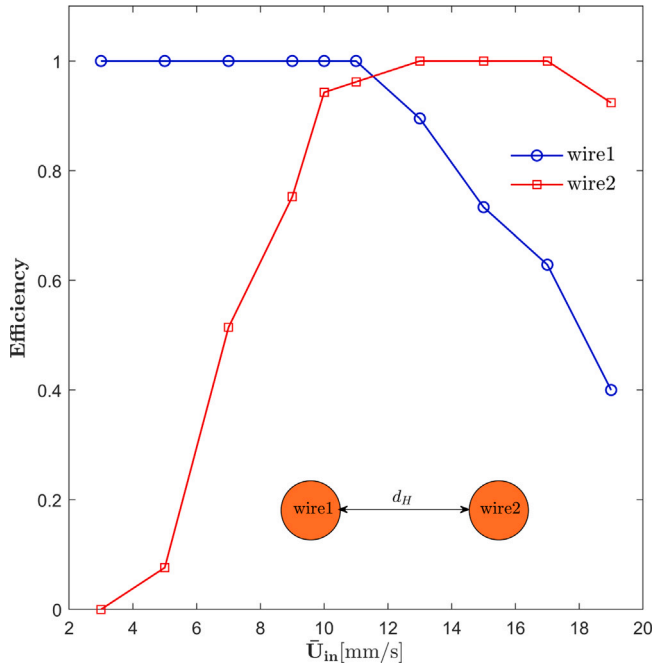

Fig. 21. Wires efficiency as a function of fluid inlet velocity; $d_H = 900\,[\mu m]$, $B_o = 0.5\,[T]$, $d_{w1} = 50\,[\mu m]$, $d_{w2} = 100\,[\mu m]$.

inlet velocity of 10 [mm/s]), the efficiency of the second wire decreases because the particles pass through the first wire and enter its repulsive zone and move away from the wires. Therefore, here is the optimization of the system for distance between the wires, which in this model for inlet velocity of 10 [mm/s] is (800 [μm] – 900 [μm]).

8.3.2. Efficiency based on inlet velocity

In the previous section, the optimal distance between the wires was calculated to maximize the efficiency of each wire. In this section, since the inlet velocity directly affects the efficiency of wires, the inlet velocity for the optimal distance between the wires is also examined and its value is determined. In this model we set wires 900 [μm] away from each other (based on last section) and increase fluid inlet velocity from 3 [mm/s] up to 19 [mm/s]. Results are shown in Fig. 21. As can be seen, when the fluid velocity is very low, the hydrodynamic force on the particles is so small that all particles are collected on the first wire and cannot pass through its attractive field. As the velocity of the fluid increases, the magnitude of the hydrodynamic force increases, and particles that are farther away from the wires and receive less magnetic force pass through the first wire and are attracted to the second wire.

It is observed that the optimal velocity in which both wires have maximum efficiency is $\bar{U}_{in} = 11\,[mm/s]$. By increasing inlet velocity, the hydrodynamic force becomes so strong that it prevents particles from being absorbed by the wires, thus reduces the efficiency of both wires.

As shown in Fig. 21, increasing the fluid velocity has a negative effect on efficiency of wire 1, so increasing the fluid velocity decreases its efficiency. In the other hand, this figure shows that increasing the fluid velocity has a positive effect on efficiency of wire 2, therefore, by increasing the fluid velocity the efficiency is increased. Thus, the point where these two lines (wire 1 efficiency and wire 2 efficiency in Fig. 21) intersect determines the optimal state of the system, which here occurs at fluid velocity 11 [mm/s]. The efficiency corresponding to this fluid velocity is 97% (vertical axis). Therefore, efficiency of the proposed system is 97%.

9. Conclusion

In this research, a microfluidic system based on magnetophoresis was designed and presented in which two ferromagnetic wires can be used to collect and separate two types of magnetic particles according to their properties (difference in diameter or difference in magnetic properties or a combination of both). These particles can be separated and collected simultaneously from a mixed inhomogeneous sample using two ferromagnetic wires.

The circular cross-section of these wires creates repulsive and attractive zones for magnetic particles. The magnetic force on the particles is directly related to their size and diameter of the wires, and this force increases with increasing particle size or wire diameter. Combining these two features, we used two wires with different sizes to collect two particle models. A smaller diameter wire is placed upstream of the channel to collect larger particles from the sample. Other wire with a larger diameter is placed downstream to collect smaller particles.

Here, the performance of this system is investigated for collecting M-280 and M450 microparticles within the microchannel. The parameters involved in this system (including wire diameter, distance between them, fluid inlet velocity, magnetic field strength and particle inlet location) were investigated separately and their value to collect each of the particles was determined. The system efficiency was obtained as a function of the distance between wires and the fluid inlet velocity.

Finally, by analyzing the results, values of the parameters were determined in order to have maximum efficiency. Using this system, we were able to separate and collect M-280 and M-450 particles with an efficiency of 97% under conditions of $\bar{U}_{in} = 11\,[mm/s]$, $d_{w1} = 50\,[\mu m]$, $d_{w2} = 100\,[\mu m]$, $B_o = 0.5\,[T]$ and y_0 in the range (200 [μm] – 300 [μm]).

In this research, our aim was to collect the two mentioned particles type and analyzed the parameters and determined their values for this particular application. All materials we have used in this research are available and values are real and there is no limit to model this system experimentally, that is our next work to do. Also, by changing some of these parameters, such as fluid inlet velocity, wires diameter or external magnetic field strength, this system can be used for other applications, for example particles or cells with different properties.

CRediT authorship contribution statement

Ali Nameni: Methodology, Software. **Mohsen Nazari:** Conceptualization, Methodology, Writing – original draft, Writing – review & editing. **Mohammad Mohsen Shahmardan:** Methodology. **Mostafa Nazari:** Methodology, Writing – original draft. **Valiollah Mashayekhi:** Conceptualization, Methodology, Writing – original draft, Writing – review & editing.

Declaration of competing interest

The authors declare that they have no known competing financial interests or personal relationships that could have appeared to influence the work reported in this paper.

References

[1] D.R. Reyes, D. Iossifidis, P.-A. Auroux, A. Manz, Micro total analysis systems. 1. Introduction, theory, and technology, Anal. Chem. 74 (12) (2002) 2623–2636, URL https://pubs.acs.org/doi/10.1021/ac0202435.

[2] M. Alshareef, N. Metrakos, E. Juarez Perez, F. Azer, F. Yang, X. Yang, G. Wang, Separation of tumor cells with dielectrophoresis-based microfluidic chip, Biomicrofluidics 7 (1) (2013) 011803, URL http://aip.scitation.org/doi/10.1063/1.4774312.

[3] A. Manz, D. Harrison, E.M. Verpoorte, J. Fettinger, A. Paulus, H. Lüdi, H. Widmer, Planar chips technology for miniaturization and integration of separation techniques into monitoring systems, J. Chromatogr. A 593 (1–2) (1992) 253–258, https://www.sciencedirect.com/science/article/pii/0021967392802934, https://linkinghub.elsevier.com/retrieve/pii/0021967392802934.

[4] S. Suresh, J. Spatz, J. Mills, A. Micoulet, M. Dao, C. Lim, M. Beil, T. Seufferlein, Connections between single-cell biomechanics and human disease states: gastrointestinal cancer and malaria, Acta Biomater. 1 (1) (2005) 15–30, URL https://linkinghub.elsevier.com/retrieve/pii/S174270610400008X.

[5] A. Vaziri, A. Gopinath, Cell and biomolecular mechanics in silico, Nature Mater. 7 (1) (2008) 15–23, URL http://www.nature.com/naturematerials, http://www.nature.com/articles/nmat2040.

[6] T. Morijiri, S. Sunahiro, M. Senaha, M. Yamada, M. Seki, Sedimentation pinched-flow fractionation for size- and density-based particle sorting in microchannels, Microfluid. Nanofluid. 11 (1) (2011) 105–110, https://www.researchgate.net/publication/226642668 http://link.springer.com/10.1007/s10404-011-0785-6.

[7] M.A. Faridi, H. Ramachandraiah, I. Banerjee, S. Ardabili, S. Zelenin, A. Russom, Elasto-inertial microfluidics for bacteria separation from whole blood for sepsis diagnostics, J. Nanobiotechnol. 15 (1) (2017) 3, URL http://jnanobiotechnology.biomedcentral.com/articles/10.1186/s12951-016-0235-4.

[8] L.R. Huang, Continuous particle separation through deterministic lateral displacement, Science 304 (5673) (2004) 987–990, https://science.sciencemag.org/content/304/5673/987.short, https://www.sciencemag.org/lookup/doi/10.1126/science.1094567.

[9] T.A. Crowley, V. Pizziconi, Isolation of plasma from whole blood using planar microfilters for lab-on-a-chip applications, Lab on a Chip 5 (9) (2005) 922, https://pubs.rsc.org/en/content/articlehtml/2005/lc/b502930a, http://xlink.rsc.org/?DOI=b502930a.

[10] N. Piacentini, G. Mernier, R. Tornay, P. Renaud, Separation of platelets from other blood cells in continuous-flow by dielectrophoresis field-flow-fractionation, Biomicrofluidics 5 (3) (2011) 034122, URL http://aip.scitation.org/doi/10.1063/1.3640045.

[11] N. Pamme, Continuous flow separations in microfluidic devices, Lab on a Chip 7 (12) (2007) 1644, URL http://xlink.rsc.org/?DOI=b712784g.

[12] A. Barani, H. Paktinat, M. Janmaleki, A. Mohammadi, P. Mosaddegh, A. Fadaei-Tehrani, A. Sanati-Nezhad, Microfluidic integrated acoustic waving for manipulation of cells and molecules, Biosens. Bioelectron. 85 (2016) 714–725, URL https://linkinghub.elsevier.com/retrieve/pii/S0956566316304870.

[13] F. Alnaimat, S. Dagher, B. Mathew, A. Hilal-Alnqbi, S. Khashan, Microfluidics based magnetophoresis: A review, Chem. Rec. 18 (11) (2018) 1596–1612, URL https://onlinelibrary.wiley.com/doi/abs/10.1002/tcr.201800018.

[14] W. Zhao, R. Cheng, S.H. Lim, J.R. Miller, W. Zhang, W. Tang, J. Xie, L. Mao, Biocompatible and label-free separation of cancer cells from cell culture lines from white blood cells in ferrofluids, Lab on a Chip 17 (13) (2017) 2243–2255, URL http://xlink.rsc.org/?DOI=C7LC00327G.

[15] Y. Zhou, D.T. Kumar, X. Lu, A. Kale, J. DuBose, Y. Song, J. Wang, D. Li, X. Xuan, Simultaneous diamagnetic and magnetic particle trapping in ferrofluid microflows via a single permanent magnet, Biomicrofluidics 9 (4) (2015) 044102, URL http://aip.scitation.org/doi/10.1063/1.4926615.

[16] N. Pamme, C. Wilhelm, Continuous sorting of magnetic cells via on-chip free-flow magnetophoresis, Lab on a Chip 6 (8) (2006) 974, https://pubs.rsc.org/en/content/articlehtml/2006/lc/b604542a, http://xlink.rsc.org/?DOI=b604542a.

[17] Z. Wang, V.B. Varma, H.M. Xia, Z.P. Wang, R.V. Ramanujan, Spreading of a ferrofluid core in three-stream micromixer channels, Phys. Fluids 27 (5) (2015) 052004, URL http://aip.scitation.org/doi/10.1063/1.4919927.

[18] T. Zhu, R. Cheng, L. Mao, Focusing microparticles in a microfluidic channel with ferrofluids, Microfluid. Nanofluid. 11 (6) (2011) 695–701, URL http://link.springer.com/10.1007/s10404-011-0835-0.

[19] K. Smistrup, T. Lund-Olesen, M.F. Hansen, P.T. Tang, Microfluidic magnetic separator using an array of soft magnetic elements, J. Appl. Phys. 99 (8) (2006) 08P102, URL http://aip.scitation.org/doi/10.1063/1.2159418.

[20] J. Kim, C.-N. Kim, Evaluation of optimization algorithms for the design of a magnetic cell separator for malaria-infected blood, J. Mech. Sci. Technol. 29 (11) (2015) 4833–4839, URL http://link.springer.com/10.1007/s12206-015-1030-0.

[21] J. Kim, H. Cho, S.-I. Han, K.-H. Han, Single-cell isolation of circulating tumor cells from whole blood by lateral magnetophoretic microseparation and microfluidic dispensing, Anal. Chem. 88 (9) (2016) 4857–4863, URL https://pubs.acs.org/doi/10.1021/acs.analchem.6b00570.

[22] J.D. Adams, U. Kim, H.T. Soh, Multitarget magnetic activated cell sorter, Proc. Natl. Acad. Sci. 105 (47) (2008) 18165–18170, https://www.pnas.org/content/105/47/18165.short, http://www.pnas.org/cgi/doi/10.1073/pnas.0809795105.

[23] Y. Zhu, B. Zhang, J. Gu, S. Li, Magnetic beads separation characteristics of a microfluidic bioseparation chip based on magnetophoresis with lattice-distributed soft magnets, J. Magn. Magn. Mater. 501 (2020) 166485, https://www.sciencedirect.com/science/article/pii/S0304885319336601, https://linkinghub.elsevier.com/retrieve/pii/S0304885319336601.

[24] N.-T. Huang, Y.-J. Hwong, R.L. Lai, A microfluidic microwell device for immunomagnetic single-cell trapping, Microfluid. Nanofluid. 22 (2) (2018) 16.

[25] K. Smistrup, O. Hansen, H. Bruus, M.F. Hansen, Magnetic separation in microfluidic systems using microfabricated electromagnets—experiments and simulations, J. Magn. Magn. Mater. 293 (1) (2005) 597–604, https://www.sciencedirect.com/science/article/pii/S0304885305001411, https://linkinghub.elsevier.com/retrieve/pii/S0304885305001411.

[26] H. Watarai, M. Namba, Capillary magnetophoresis of human blood cells and their magnetophoretic trapping in a flow system, J. Chromatogr. A 961 (1) (2002) 3–8.

[27] P.-L. Guo, M. Tang, S.-L. Hong, X. Yu, D.-W. Pang, Z.-L. Zhang, Combination of dynamic magnetophoretic separation and stationary magnetic trap for highly sensitive and selective detection of Salmonella typhimurium in complex matrix, Biosens. Bioelectron. 74 (2015) 628–636.

[28] M. Eshaghi, M. Nazari, M. Shahmardan, M. Ramezani, V. Mashayekhi, Particle separation in a microchannel by applying magnetic fields and Nickel Sputtering, J. Magn. Magn. Mater. 514 (2020) 167121, https://www.sciencedirect.com/science/article/pii/S0304885320309616, https://linkinghub.elsevier.com/retrieve/pii/S0304885320309616.

[29] Q. Ramadan, D.P. Poenar, C. Yu, Customized trapping of magnetic particles, Microfluid. Nanofluid. 6 (1) (2009) 53–62.

[30] X. Xuan, J. Zhu, C. Church, Particle focusing in microfluidic devices, Microfluid. Nanofluid. 9 (1) (2010) 1–16, URL http://link.springer.com/10.1007/s10404-010-0602-7.

[31] C.D. James, J. McClain, K.R. Pohl, N. Reuel, K.E. Achyuthan, C.J. Bourdon, K. Rahimian, P.C. Galambos, G. Ludwig, M.S. Derzon, High-efficiency magnetic particle focusing using dielectrophoresis and magnetophoresis in a microfluidic device, J. Micromech. Microeng. 20 (4) (2010) 045015, https://iopscience.iop.org/article/10.1088/0960-1317/20/4/045015/meta, https://iopscience.iop.org/article/10.1088/0960-1317/20/4/045015.

[32] S.A. Peyman, E.Y. Kwan, O. Margarson, A. Iles, N. Pamme, Diamagnetic repulsion—A versatile tool for label-free particle handling in microfluidic devices, J. Chromatogr. A 1216 (52) (2009) 9055–9062, https://www.sciencedirect.com/science/article/pii/S0021967309009212, https://linkinghub.elsevier.com/retrieve/pii/S0021967309009212.

[33] Q. Cao, Z. Li, Z. Wang, F. Qi, X. Han, Disaggregation and separation dynamics of magnetic particles in a microfluidic flow under an alternating gradient magnetic field, J. Phys. D: Appl. Phys. 51 (19) (2018) 195002.

[34] S.A. Khashan, S. Dagher, A. Alazzam, Microfluidic multi-target sorting by magnetic repulsion, Microfluid. Nanofluid. 22 (6) (2018) 64.

[35] X. Han, Y. Feng, Q. Cao, L. Li, Three-dimensional analysis and enhancement of continuous magnetic separation of particles in microfluidics, Microfluid. Nanofluid. 18 (5–6) (2015) 1209–1220, https://link.springer.com/article/10.1007/s10404-014-1516-6, http://link.springer.com/10.1007/s10404-014-1516-6.

[36] E.M. Purcell, D.J. Morin, Electricity and Magnetism, Cambridge University Press, 2013.

[37] K.-H. Han, A. Bruno Frazier, Continuous magnetophoretic separation of blood cells in microdevice format, J. Appl. Phys. 96 (10) (2004) 5797–5802.

[38] S.A. Khashan, S. Dagher, A. Alazzam, Microfluidic multi-target sorting by magnetic repulsion, Article Microfluid. Nanofluid. 22 (6) (2018) URL http://dx.doi.org/10.1007/s10404-018-2083-z.

[39] B.R. Munson, T.H. Okiishi, W.W. Huebsch, A.P. Rothmayer, Fluid Mechanics, Wiley Singapore, 2013.

[40] A. Kovetz, The Principles of Electromagnetic Theory, CUP Archive, 1990.